

# Tuning the hydrogen desorption of $\text{Mg}(\text{BH}_4)_2$ through Zn alloying

D. Harrison and T. Thonhauser\*

*Department of Physics, Wake Forest University, Winston-Salem, NC 27109, USA.*

(Dated: November 4, 2018)

We study the effect of Zn alloying on the hydrogen desorption properties of  $\text{Mg}(\text{BH}_4)_2$  using *ab initio* simulations. In particular, we investigate formation/reaction enthalpies/entropies for a number of compounds and reactions at a wide range of temperatures and Zn concentrations in  $\text{Mg}_{1-x}\text{Zn}_x(\text{BH}_4)_2$ . Our results show that the thermodynamic stability of the resulting material can be significantly lowered through Zn alloying. We find that e.g. the solid solution  $\text{Mg}_{2/3}\text{Zn}_{1/3}(\text{BH}_4)_2$  has a reaction enthalpy for the complete hydrogen desorption of only 25.3 kJ/mol  $\text{H}_2$ —a lowering of 15 kJ/mol  $\text{H}_2$  compared to the pure phase and a corresponding lowering in critical temperature of 123 K. In addition, we find that the enthalpy of mixing is rather small and show that the decrease in reaction enthalpy with Zn concentration is approximately linear.

PACS numbers: 63.20.dk, 65.40.-b, 61.50.Ah

## I. INTRODUCTION

Metal borohydrides are amongst the most promising hydrogen storage materials,<sup>1–5</sup> as they have some of the highest storage densities. Unfortunately, the hydrogen desorption temperature for the most attractive borohydrides is too high for on-board storage, where it should be below 85°C.<sup>6,7</sup> Thus, borohydrides have been studied intensely in order to lower their desorption temperature. Destabilizing via reactions with other hydrides has been suggested,<sup>8–11</sup> as well as simple doping,<sup>12,13</sup> cation substitution,<sup>14</sup> anion substitution,<sup>15</sup> or adding catalysts<sup>16</sup>—but unfortunately, the results still fall short of the required DOE targets.<sup>6</sup>

The borohydride  $\text{Mg}(\text{BH}_4)_2$  is of particular interest; it has substantial storage density of 14.9 mass% and its decomposition has been shown to be fully reversible under certain conditions,<sup>17</sup> but it completes its first major intermediate step around 570 K and doesn't fully desorb until it reaches temperatures around 820 K.<sup>11,18</sup> If we can lower its desorption temperature, it might be one of the few materials to satisfy the DOE targets. The desorption temperature is determined by the thermodynamics and kinetics of the desorption reaction. Although it is generally believed that kinetics is the “culprit” in the case of  $\text{Mg}(\text{BH}_4)_2$ ,<sup>19</sup> it is still desirable to first optimize the thermodynamics before addressing the kinetic barrier.<sup>10</sup> In the present manuscript, we investigate the thermodynamics of the desorption of  $\text{Mg}(\text{BH}_4)_2$  and the dramatic effect Zn alloying has on it.

We have recently become aware of some very nice work also studying Mg/Zn borohydride solid solutions, and will use this opportunity to compare our results with theirs and point out similarities and differences.<sup>20</sup> Further simulations have been performed studying the desorption of  $\text{Mg}(\text{BH}_4)_2$ ,<sup>21,22</sup> but without accounting for van der Waals contributions, known to be necessary to achieve the correct energetic ordering among polymorphs of  $\text{Mg}(\text{BH}_4)_2$ ;<sup>23,24</sup> we will thus compare our results of the desorption pathway with other works to ascertain the ef-

fect of van der Waals interactions. We also argue that given the minimum practical delivery pressure from storage system of 3 bar, the overall desorption reaction is, in fact, outside the ideal thermodynamic window of  $-40^\circ\text{C}$  to  $+85^\circ\text{C}$ ,<sup>6</sup> but can be brought there by alloying with Zn. We also find a linear relationship between the overall hydrogen desorption enthalpy and Zn concentration in  $\text{Mg}(\text{BH}_4)_2$ .

Borohydrides are complex hydrides, in which tetrahedral anion units, such as  $[\text{BH}_4]^-$  and  $[\text{AlH}_4]^-$ , are bound to more electropositive cations, such as Li, Na, K, Mg, and Ca. The ionic bonding and charge transfer between the cations and the anion units is a key feature of the stability of these hydrides.<sup>25</sup> Targeting this feature, the desorption temperature of  $\text{Mg}_2\text{NiH}_4$  was successfully lowered by destabilizing it through cation substitution.<sup>14</sup> The same can also be achieved by altering the anion complex, as demonstrated with fluorine substitution in the hydrogen sublattice of  $\text{Na}_3\text{AlH}_6$ .<sup>1,15</sup> More generally, an extensive experimental study revealed an almost linear correlation between the desorption temperature  $T_d$  in K and the Pauling electronegativity  $\chi_P$  as well as the hydrogen desorption reaction enthalpy  $\Delta H_r$  in kJ/mol  $\text{H}_2$ :<sup>26</sup>

$$T_d = 1234 - 517.3 \chi_P, \quad (1)$$

$$T_d = 423.4 + 8.34 \Delta H_r. \quad (2)$$

The study included data for  $\mathcal{M}(\text{BH}_4)_n$  with  $\mathcal{M} = \text{Li}, \text{Na}, \text{K}, \text{Mg}, \text{Zn}, \text{Sc}, \text{Zr},$  and  $\text{Hf}$ ,<sup>25</sup> and was later extended by Ca, Ti, V, Cr, and Mn.<sup>27</sup>  $\text{Zn}(\text{BH}_4)_2$  stands out in that it has the lowest temperature for full decomposition of only 410 K.<sup>28</sup>  $\text{Zn}(\text{BH}_4)_2$  itself is thermodynamically unstable at room temperature and produces diborane gases in its decomposition reaction—it is thus not directly interesting for hydrogen storage. But, as we will argue below, Zn is an ideal alloyant for the  $\text{Mg}(\text{BH}_4)_2$  system, forming  $\text{Mg}_{1-x}\text{Zn}_x(\text{BH}_4)_2$ , with remarkable effects. Zn alloying of  $\text{Mg}(\text{BH}_4)_2$  is supported by the following facts: (i) Zn alloying has been found experimentally to significantly lower the decomposition temperature;<sup>20,29</sup> (ii) Zn alloying lowers the decomposition temperature

of other borohydrides;<sup>30</sup> (iii) Zn is known to form a borohydride with the same stoichiometry as  $\text{Mg}(\text{BH}_4)_2$  and their structures are essentially the same<sup>25</sup> (the ionic radii of Zn and Mg of 0.88 and 0.86 Å are virtually identical); (iv) alloying in other borohydrides, such as  $\text{Li}_{1-x}\text{Cu}_x\text{BH}_4$ , shows a desorption temperature between the two constituents;<sup>12,31</sup> (v) Zn is known to not form hydrides or borides like other borohydrides,<sup>25</sup> simplifying the hydrogen desorption reaction significantly; and finally (vi) Zn is an abundant major industrial metal.

## II. COMPUTATIONAL DETAILS

In order to study the thermodynamics of  $\text{Mg}(\text{BH}_4)_2$  and the effect of Zn alloying, we need the enthalpies and entropies for all materials suspected in the decomposition of  $\text{Mg}(\text{BH}_4)_2$ . To this end, we performed *ab initio* simulations at the DFT level, as implemented in VASP,<sup>32,33</sup> to calculate the ground-state energies and phonon densities of states. We used PAW pseudopotentials with a 650 eV kinetic energy cutoff and an energy convergence criterion of  $10^{-7}$  eV. We used  $k$ -point meshes giving convergence to within 1 meV/atom, with the exception of the metallic compounds and elemental boron, which were converged to within 3 meV/atom. This yielded a  $k$ -point mesh of e.g.  $5 \times 5 \times 4$  for small unit cells like  $\text{MgB}_2$  and a mesh of  $1 \times 1 \times 1$  for large unit cells like  $\text{Mg}(\text{BH}_4)_2$ . Structures were relaxed with respect to unit-cell parameters and atom positions until all forces were less than 0.1 meV/Å. This way, we found the lowest-energy structure of boron to be the 106 atom  $\beta$ -rhombohedral structure suggested by van Setten et al.<sup>34</sup> Phonons were calculated with the symmetry-reduced finite-displacement method with displacements of 0.015 Å. Supercells were created such that they were the same dimensions as the  $k$ -point mesh used for the original unit cell. The exceptions were the metals Mg and Zn, whose phonons were calculated with a  $5 \times 5 \times 2$  supercell and a  $3 \times 3 \times 4$   $k$ -point mesh.

While the ground-state structure of  $\text{Mg}(\text{BH}_4)_2$  is experimentally known to be of  $P6_122$  symmetry with 30 formula units per unit cell, theoretical studies with a variety of exchange-correlation (XC) functionals find numerous other structures, all disagreeing with experiment.<sup>24</sup> The reason for this is that  $\text{Mg}(\text{BH}_4)_2$ —similar to other borohydrides<sup>35</sup>—exhibits a small but important contribution from van der Waals interactions, on the order of 0.1 eV per  $\text{BH}_4$  unit. Including those contributions via the XC functional vdW-DF<sup>36,37</sup>—with the (semi)local XC as originally defined in Ref. [38]—we were the first to find the correct ground-state structure in agreement with experiment.<sup>24</sup> We further found that the closely related  $P3_112$  structure is less than 1 meV per atom higher in energy. This structure has only 9 formula units per unit cell and the local coordination is almost identical to the  $P6_122$  structure, resulting in almost identical phonon densities of states. Thus, in the present study we are using vdW-DF and the numerically feasible  $P3_112$  struc-

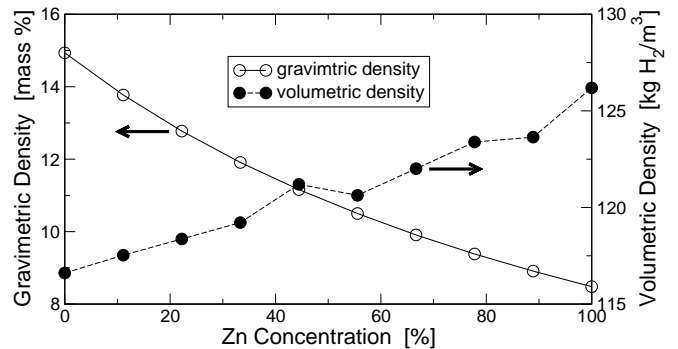


FIG. 1.  $\text{H}_2$  gravimetric storage density in mass% (to be read off the left axis) and  $\text{H}_2$  volumetric storage density in  $\text{kg H}_2/\text{m}^3$  (right axis) for different Zn concentrations.

ture for all our simulations. This is further justified by comparing one of our reaction enthalpies to the results of Albanese et al. in Ref. [20], who in fact used the large  $P6_122$  structure and obtained almost identical results—see details below. As our structure has 9 formula units per unit cell, we report results for Zn concentrations in steps of 1/9. Alloying was done by randomly replacing Mg atoms with Zn, with variations—due to which atoms are being replaced—being on the order of only fractions of a kJ/mol at the most. Our results for the enthalpy of mixing compare well with Albanese et al., who found similarly small values.<sup>20</sup>

## III. RESULTS

### A. Storage Densities

The gravimetric storage density of  $\text{Mg}(\text{BH}_4)_2$  will decrease with increasing Zn content, as can be seen in Fig. 1. But, as we shall see below, only modest alloying is necessary to achieve the required effect, and the loss in gravimetric density is reasonable. On the other hand, the volumetric density increases with increasing Zn content. The “bump” or deviation from linear behavior, observed in Fig. 1 around 50% Zn concentration, is also seen in the work of Albanese et al.,<sup>20</sup> and may be indicative of the formation of a superstructure.

### B. Structural Stability and Ionic Character

We begin by analyzing the structural stability in terms of the ionic character as a function of Zn concentration. As mentioned above, the ionic bonding is a key feature of the stability of borohydrides. In Table I we quantify this picture and present a Bader charge analysis as a function of Zn concentration, using the fast implementation proposed by Henkelman et al.<sup>39</sup> Note that the Bader analysis, similarly to the Mulliken analysis, is an intuitive (but not unique) way of partitioning the electron charge.

TABLE I. Bader charges (in units of  $e$ ) for the metal site  $\mathcal{M}$  and the  $\text{BH}_4$  units as a function of concentration  $x$  in  $\text{Mg}_{1-x}\text{Zn}_x(\text{BH}_4)_2$ . Given are also the Pauling electronegativity  $\chi_P$  and the estimated desorption temperature  $T_d$  (in K) from Eq. (1). The reported charges and electronegativities are values averaged over all 9 formula units in the unit cell.

$x$	0	1/9	2/9	3/9	4/9	5/9	6/9	7/9	8/9	1
$\mathcal{M}$	+1.72	+1.65	+1.59	+1.53	+1.46	+1.40	+1.33	+1.26	+1.20	+1.13
$\text{BH}_4$	-0.86	-0.83	-0.79	-0.76	-0.73	-0.70	-0.67	-0.63	-0.60	-0.56
$\chi_P$	1.20	1.24	1.29	1.33	1.38	1.42	1.47	1.51	1.56	1.60
$T_d$	613	593	567	546	520	499	474	453	427	406

Interestingly, even for the pure  $\text{Mg}(\text{BH}_4)_2$  structure, the ionic character significantly deviates from the nominal values of +2 and -1. As expected, the ionic character diminishes as a function of Zn concentration due to the higher electronegativity of Zn, approximately 0.06  $e$  per 10% Zn. A more detailed analysis of the charge density reveals the following: While the direct effect of Zn is localized, hydrogens further away from Zn get a small compensating charge if they are within a tetrahedra next to a Zn. Through this mechanism, even low levels of alloying influence almost the entire structure. In Table I we also show the Pauling electronegativity  $\chi_P$  as a function of Zn concentration and the corresponding estimated desorption temperatures  $T_d$  according to Eq. (1). Purely based on this experimentally found connection for borohydrides, we can already estimate that modest Zn alloying might reduce the desorption temperature on the order of 100 K. In the remainder of this paper, we will quantify this empirical estimate.

### C. Thermodynamics of the Hydrogen Desorption at 1 Bar Hydrogen Pressure

We now move to the main point of this paper, i.e. the thermodynamics of the hydrogen desorption and the effect of Zn alloying. To this end, we calculate the temperature dependent vibrational contribution to the enthalpy and entropy as

$$H_{\text{vib}} = \int_0^\infty d\omega \left( \frac{1}{2} + \frac{1}{\exp[\hbar\omega/kT] - 1} \right) g(\omega) \hbar\omega, \quad (3)$$

$$S_{\text{vib}} = \int_0^\infty d\omega \left( \frac{\hbar\omega}{2T} \coth \frac{\hbar\omega}{2kT} - k \ln \left[ 2 \sinh \frac{\hbar\omega}{2kT} \right] \right) g(\omega), \quad (4)$$

where  $\omega$  is the vibrational frequency,  $g(\omega)$  is the phonon density of states,  $T$  is the temperature, and  $k$  is Boltzmann's constant. The enthalpy then is the sum of the DFT ground-state energy and this vibrational contribution. Formation enthalpies, in turn, are calculated as differences in enthalpies of the material and its constituent elements (thus, elements in their natural state have formation enthalpies of 0). From this, we calculate enthalpies and entropies of reaction, using formation enthalpies and absolute entropies of all materials (tabulated in the appendix). For reactions involving Zn alloying (Reactions 2, 3, and 13 in Table II), the entropy of

mixing was calculated according to

$$S_{\text{mix}} = -k_B [c \ln c + (1 - c) \ln (1 - c)], \quad (5)$$

where  $c$  is the concentration of Zn; this entropy of mixing was added to the entropy of reaction calculated from vibrational frequencies, resulting in e.g. a decrease in reaction entropy of  $\sim 5$  J/K/mol  $\text{H}_2$  and a corresponding increase in the critical temperature of  $\sim 10$  K. Note that all structures we found are true local minima and none of the density of states show imaginary frequencies.

Following the approach of van Setten et al.,<sup>22</sup> the temperature-dependent thermodynamic values of  $\text{H}_2$  were obtained using experimental data.<sup>40</sup> In particular, we used  $H_{\text{H}_2 \text{ gas}}(T) = E_{\text{H}_2} + E_{\text{H}_2}^{\text{ZPE}} + H_{\text{H}_2 \text{ gas}}^{\text{exp}}(T)$ , where the electronic energy  $E_{\text{H}_2}$  and zero-point energy  $E_{\text{H}_2}^{\text{ZPE}}$  were calculated using DFT and the last term was taken from experiment.<sup>40</sup> Specifically, data was taken from  $\text{H}_2$  at 1 bar for increments of 100 K with values in between being linearly interpolated. Note that the enthalpy of  $\text{H}_2$  changes very little over moderate pressure changes (e.g. the change in enthalpy going from 1 to 100 bar at 300 K is only 0.114 kJ/mol), meaning our formation enthalpies should be useful even when looking at high pressures. The entropy of hydrogen gas used to calculate the entropies of reaction in Table II and the reactions at 3 bar discussed later on were likewise taken from the same experimental data.<sup>40</sup> For reference, the entropies of  $\text{H}_2$  at 300 K for 1 and 3 bar are 130.77 and 121.63 J/K/mol  $\text{H}_2$ , respectively. Note that the entropy of hydrogen gas for other pressures can be accurately estimated by the equation  $S_{\text{H}_2} = -R \ln p + S_0$ , where  $p$  is the pressure in bar and  $S_0$  is the entropy at 1 bar.

The overall energy required for the hydrogen decomposition reaction to start can be split into two pieces, i.e. the *reaction enthalpy* and an additional *kinetic barrier*. We argue that the latter is similar for the initial hydrogen release of many decomposition reactions of borohydrides and focus first on the reaction enthalpies. Table II contains the most pertinent results from this study; it lists reaction enthalpies for a number of possible reactions, calculated from formation enthalpies for a range of materials. Where a direct comparison with experiment is possible, we generally find very good agreement. For example, experimental formation enthalpies for  $\text{MgH}_2$  and  $\text{MgB}_2$  of -75.3 and -41.2 kJ/mol are in excellent agreement with our calculated values of -78.7 and -43.4 kJ/mol (see appendix A).<sup>42,43</sup> Furthermore,

TABLE II. Reaction enthalpies  $\Delta H_r$  in kJ/mol  $H_2$  and entropies  $\Delta S_r$  in J/K/mol  $H_2$  at 300 K for several  $Mg(BH_4)_2$  desorption reactions. The critical temperature  $T_c$  predicted from the van't Hoff equation  $\ln p = -\Delta H/RT + \Delta S/R$  for 1 bar  $H_2$  pressure is given in K. We give a rough estimate of the kinetic barrier in K as the difference  $T_{\text{barrier}} = T_d - T_c$ , where  $T_d$  is the approximate experimental desorption temperature.

No.	Reactants	→	Products	$\Delta H_r^{300K}$	$\Delta S_r^{300K}$	$T_c$	$T_d$	$T_{\text{barrier}}$
1	$Mg(BH_4)_2$	→	$MgB_2 + 4H_2$	40.3	112.15	360	820 <sup>a</sup>	460
2	$Mg_{2/3}Zn_{1/3}(BH_4)_2$	→	$\frac{2}{3}MgB_2 + \frac{1}{3}Zn + \frac{2}{3}B + 4H_2$	25.3	106.72	237		
3	$Mg_{1/3}Zn_{2/3}(BH_4)_2$	→	$\frac{1}{3}MgB_2 + \frac{2}{3}Zn + \frac{1}{3}B + 4H_2$	10.4	106.57	98		
4	$Zn(BH_4)_2$	→	$Zn + 2B + 4H_2$	-3.92	112.57	-35	410 <sup>b</sup>	445
5	$Mg(BH_4)_2$	→	$\frac{1}{6}MgB_{12}H_{12} + \frac{5}{6}MgH_2 + \frac{13}{6}H_2$	24.8	104.71	237	570 <sup>c</sup>	333
6	$MgH_2$	→	$Mg + H_2$	78.7	132.99	592	640 <sup>d</sup>	48
7	$\frac{1}{6}MgB_{12}H_{12}$	→	$\frac{1}{6}Mg + 2B + H_2$	85.4	119.30	716	730 <sup>d</sup>	14
8	$Mg(BH_4)_2$	→	$\frac{1}{6}MgB_{12}H_{12} + \frac{5}{6}Mg + 3H_2$	39.8	112.56	353		
9	$\frac{1}{6}MgB_{12}H_{12} + \frac{5}{6}Mg$	→	$MgB_2 + H_2$	42.0	110.91	379		
10	$\frac{1}{6}MgB_{12}H_{12}$	→	$\frac{1}{6}MgH_2 + 2B + \frac{5}{6}H_2$	86.8	116.56	744		
11	$\frac{1}{6}MgB_{12}H_{12} + \frac{5}{6}MgH_2$	→	$\frac{1}{2}MgB_4 + \frac{1}{2}MgH_2 + \frac{4}{3}H_2$	63.5	121.13	525		
12	$Mg(BH_4)_2$	→	$MgH_2 + 2B + 3H_2$	42.0	108.00	389		
13	$Mg_{4/5}Zn_{1/5}(BH_4)_2$	→	$\frac{4}{5}MgH_2 + \frac{1}{5}Zn + 2B + \frac{16}{5}H_2$	30.5	104.98	291		

<sup>a</sup>Ref. [18]; <sup>b</sup>Ref. [28]; <sup>c</sup>Ref. [41]; <sup>d</sup>Ref. [11].

our calculated reaction enthalpies for Reactions 1 and 8 of 40.3 kJ/mol  $H_2$  and 39.8 kJ/mol  $H_2$  are also in good agreement with the value of  $40 \pm 2$  kJ/mol  $H_2$  found by Yan et al. in Ref. [41].<sup>44</sup> Previous theoretical studies have calculated an overall reaction enthalpy of 38–39 kJ/mol  $H_2$  at room temperature,<sup>19,21,22,45</sup> which closely agrees with our value of 40.3 kJ/mol  $H_2$ . We attribute the difference to vdW-DF, which stabilizes  $Mg(BH_4)_2$  with respect to its reaction products by accounting for the long-range van der Waals forces. Comparison of our results for other decomposition reactions with previous studies shows similar agreement, with differences on the order of several kJ/mol  $H_2$  due to vdW-DF. Although accounting for long-range van der Waals forces has been found to be critical to finding the correct energetic ordering among polymorphs in borohydrides,<sup>23,24</sup> it seems to affect total reaction enthalpies by only several kJ/mol  $H_2$  at the most.

Reactions 1 – 4 of Table II show the effects of Zn alloying on the overall reaction enthalpy. We find the effect to be linear and every 10% Zn results in a further lowering of the desorption enthalpy by approximately 4.5 kJ/mol  $H_2$ , as can be seen in Fig. 2. Zn alloying thus provides a convenient way of tuning the desorption enthalpy over a wide range. Note that the desorption enthalpy of Reactions 2 and 5 are approximately the same, but the important difference is that the alloyed phase releases the entire hydrogen, while the latter only releases half of the available hydrogen. Furthermore, note that Reactions 1 – 4 are different from the decomposition modeled in Ref. [20] in that we model the entire hydrogen release, i.e. the outcome is  $MgB_2 + 4H_2$ , whereas they assume the intermediate  $MgH_2$ . For comparison, we have modeled their reaction also (Reaction 13 in Table II), obtaining 30.5 kJ/mol  $H_2$  in excellent agreement to their value of 30 kJ/mol  $H_2$ —in fact, justifying approximations that both our groups have made. It is important

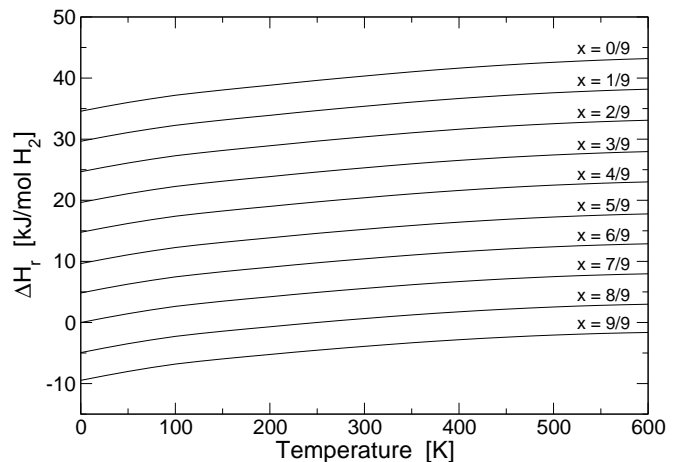


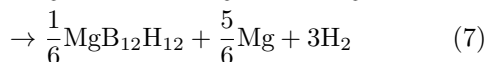
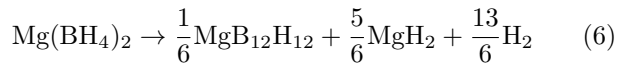
FIG. 2. Reactions enthalpies  $\Delta H_r$  can readily be calculated from the tabulated data in the appendices. As an example, we plot here the reaction enthalpy as a function of temperature and alloying for the reaction  $Mg_{1-x}B_2(1-x) + Zn_x + 2B_x + 4H_2$ . Note that the effect of Zn concentration on the reaction enthalpy is almost perfectly linear.

to also compare the two corresponding “pure” reactions, i.e. Reaction 1 and 12. The reaction enthalpy for the entire hydrogen release in Reaction 1 is, in fact, a little lower compared to Reaction 12, which led us to pursue the pure reaction pathway.

Note that we did not list the effects of Zn alloying on intermediate reactions because it was unknown whether Zn would remain in  $MgB_{12}H_{12}$  or phase separate, and in either case there was no experimental data on the corresponding structures. Reactions 5 – 7 show suspected intermediate steps, while Reactions 8 – 13 show alternative reactions discussed later; data for other possible

reactions can be readily calculated using extensive thermodynamic data tabulated in the appendix.

Of course, it is also well known that there are more intermediates in the decomposition of  $\text{Mg}(\text{BH}_4)_2$  involving  $\text{Mg}(\text{B}_x\text{H}_y)_z$  complexes,<sup>19,46</sup> especially in the formation and decomposition of  $\text{MgB}_{12}\text{H}_{12}$ . While we did not study all of these possible intermediates, our calculated thermodynamic values in the appendix can give insight into some other favorable pathways. Within the framework of pathways considered, our results show that the most favorable pathway for hydrogen desorption that agrees with experiment is:



Thermodynamically, as seen in Reaction 9, the most favorable pathway after the formation of  $\text{MgB}_{12}\text{H}_{12}$  is the formation of  $\text{MgB}_2$ , but from experimental differential scanning calorimetry and chemical intuition, it is likely that there is at least one intermediate step from  $\text{MgB}_{12}\text{H}_{12}$  to  $\text{MgB}_2$ . The theoretical total hydrogen loss for steps (6), (7), and (9) is 8.1%, 11.2%, and 14.9%, respectively. The formation of  $\text{MgB}_{12}\text{H}_{12}$ ,  $\text{MgH}_2$ ,  $\text{Mg}$ , and  $\text{MgB}_2$  are all well-known steps confirmed by X-ray diffraction and solid state NMR.<sup>11,18,47,48</sup> They are also supported as thermodynamically favorable by a number of theoretical studies.<sup>21,49</sup> Furthermore, the temperature evolution of the reaction products also supports this reaction pathway:  $\text{MgH}_2$  appears first, then  $\text{Mg}$  without  $\text{MgH}_2$ , and finally  $\text{MgB}_2$ .

Equation (6) also corresponds to the mass% of hydrogen desorbed for certain temperatures held for long periods of time. Yan et al. found that just over 8 mass% of  $\text{H}_2$  desorb after 1000 min at 573 K; this corresponds almost exactly to the expected value of 8.1% for Eq. (6).<sup>47</sup> It is also worth noting that it took over an hour before even 4 mass% of  $\text{H}_2$  was desorbed, and the curves for lower temperatures never equilibrated after 1000 min. Due to the sluggish kinetics of this step of the reaction it is difficult to see the individual reaction steps in a typical thermogravimetry curve; by the time only a fraction of  $\text{Mg}(\text{BH}_4)_2$  has undergone the first step of the reaction, the temperature has increased so that the second step of the reaction has already begun. However, we can see further evidence for the proposed reaction pathway by the results of Matsunaga et al., who found that  $\text{Mg}(\text{BH}_4)_2$  could be rehydrogenated from 11% to 8% at 623 K, which corresponds to the rehydrogenation of  $\text{Mg}$  to  $\text{MgH}_2$  (see Fig. 6 of Ref. [50]).

We also find that the previously suggested decomposition of  $\text{MgB}_{12}\text{H}_{12}$  to  $\text{MgH}_2$  and elements shown in Reaction 10 to be unfavorable as a second step of the reaction, with a critical temperature of 744 K, and suggest the decomposition of  $\text{MgH}_2$  ( $T_c = 592$  K) as occurring before

$\text{MgB}_{12}\text{H}_{12}$ . After  $\text{MgH}_2$  decomposes, we suggest the decomposition of  $\text{MgB}_{12}\text{H}_{12}$  as our critical temperature of 716 K coincides closely with the final large dip observed in differential scanning calorimetry plots near 1 bar  $\text{H}_2$  pressure.<sup>41</sup> Finally, we find the formation of  $\text{MgB}_4$  to be plausible, as evidenced by the favorable thermodynamics of Reaction 11.

Reaction 13 is the decomposition reaction modeled by Albanese et al. as having the optimal decomposition enthalpy;<sup>20</sup> our calculated value of 30.5 kJ/mol  $\text{H}_2$  is in exact agreement with their result of 30 kJ/mol  $\text{H}_2$ . Note that our enthalpy and entropy used for 20% Zn-alloyed  $\text{Mg}(\text{BH}_4)_2$  were calculated from a linear interpolation of our thermodynamic data; this is valid because the change in enthalpy and entropy values with Zn concentration is nearly exactly linear (see the appendix). It is interesting to see that, when we interpolate our results for Reactions 1 – 4 to a Zn concentration of 1/5 to match the concentration in Reaction 13, we find a reaction enthalpy and entropy of 31.46 kJ/mol  $\text{H}_2$  and 112 J/K/mol  $\text{H}_2$ , leading to a critical temperature  $T_c = 281$  K, which is essentially the same as for Reaction 13 in Table II. Although our results for Reaction 13 agree with the work done by Albanese et al., our work can be seen as an extension of the theoretical part of that study, as we have actually calculated the full thermodynamic data—including reaction entropies—instead of interpolating them. We have done so for their proposed partial decomposition (Reaction 13) and in addition for a large number of other reactions (Reactions 1 – 11), including the full hydrogen decomposition as well as others that can easily be deduced from the tabulated thermodynamic data in our appendix.

#### D. Thermodynamics of the Hydrogen Desorption at 3 Bar Hydrogen Pressure

From the results above it follows that kinetics is not the only problem with  $\text{Mg}(\text{BH}_4)_2$ , as the reaction from  $\text{Mg}(\text{BH}_4)_2$  to  $\text{MgB}_2$  has a calculated critical temperature of 360 K (86°C). Note that this critical temperature was calculated at 1 bar  $\text{H}_2$  pressure, while the minimum DOE target for delivery pressure is around 3 bar; the critical temperature at 3 bar is 430 K (157°C), well outside the optimal thermodynamic window. Furthermore, while Zuttel et al. have argued that the entropic contribution to metal hydride reactions is approximately 130 J/K/mol  $\text{H}_2$  for most simple metal-hydrogen systems,<sup>51</sup> lower values can occur for complex metal hydrides, such as 97 J/K/mol  $\text{H}_2$  for  $\text{LiBH}_4 \rightarrow \text{LiH} + \text{B} + 3/2\text{H}_2$ .<sup>9</sup> It seems likely then that  $\text{Mg}(\text{BH}_4)_2$  also has a lower than normal entropy of reaction, in agreement with our calculated values in Table II, given its similarity to  $\text{LiBH}_4$ . Because of this comparatively low value for the reaction entropy, even the commonly cited value of 40 kJ/mol  $\text{H}_2$  is too high for a practical PEM fuel cell. In fact, using our calculated entropy

value, for a minimum delivery pressure of 3 bar and temperature of 80°C, the maximum desired enthalpy is 33 kJ/mol H<sub>2</sub>. Also note that while the estimated desired reaction enthalpy for a hydrogen storage material is 20–50 kJ/mol H<sub>2</sub> (for reactions with low to high entropic contributions), the ideal range for efficiency is 20–30 kJ/mol H<sub>2</sub>.<sup>7</sup> All of this points towards the conclusion that Mg(BH<sub>4</sub>)<sub>2</sub> needs to be destabilized with respect to its reaction products in order to achieve the ideal thermodynamic reaction window. E.g. in the case of 1/3 Zn alloying, we find a reaction enthalpy of 25.3 kJ/mol H<sub>2</sub> and a critical temperature of 270 K (−3°C) at 3 bar, both in the ideal range for a PEM fuel cell. This is based on the suspected decomposition reaction  $\text{Mg}_{1-x}\text{Zn}_x(\text{BH}_4)_2 \rightarrow \text{Mg}_{1-x}\text{B}_{2(1-x)} + \text{Zn}_x + 2\text{B}_x + 4\text{H}_2$ . We find this to be the most likely reaction as Zn(BH<sub>4</sub>)<sub>2</sub> “decomposes directly to elemental Zn due to instabilities of Zn hydride and boride,”<sup>25</sup> and we find Zn-alloyed MgB<sub>2</sub> to be unstable and expect it to phase separate to MgB<sub>2</sub>, Zn, and B based on preliminary calculations. Of course, for high concentrations of Zn, we expect the formation of diborane, as seen experimentally by Albanese et al. and Kalantzopoulos et al.,<sup>20,29</sup> but for low concentrations of Zn it is known that diborane is not formed.

### E. Kinetics of the Hydrogen Desorption and overall Desorption Temperature

We now switch to a discussion of the kinetic barrier. By comparing our calculated critical temperatures  $T_c$  with the known experimental temperatures of hydrogen desorption  $T_d$ ,<sup>11,18,28,47</sup> we can make a rough estimate of the kinetic barrier, given in Table II. Interestingly, from Eq. (2) we see that—by definition—borohydrides with  $\Delta H_r = 0$  have a kinetic barrier of 423.4 K; using the same argument but a slightly different fit (see footnote 26), we find a kinetic barrier of 439.4 K. Borohydrides with  $\Delta H_r \approx 0$ , such as Zn(BH<sub>4</sub>)<sub>2</sub>, thus must have a kinetic barrier of the same order of magnitude, in very good agreement to our calculated value of 445 K for Zn.

From Table II we see that the kinetic barrier for the full hydrogen release reaction is almost the same for Mg(BH<sub>4</sub>)<sub>2</sub> and Zn(BH<sub>4</sub>)<sub>2</sub>, which in turn means that differences in calculated critical temperatures in Table II approximately result in the same differences for the overall desorption temperature. We thus estimate a decrease of desorption temperature of Mg(BH<sub>4</sub>)<sub>2</sub> when alloying with Zn for Reaction 1 of approximately 123 K for 1/3 Zn concentration and 262 K for 2/3 Zn. Note that we obtain almost identical numbers using a different argument: Simply evaluating the experimental relationship in Eq. (2), purely based on our calculated changes in enthalpy, gives a lowering of the desorption temperature of

125 K for 1/3 Zn concentration and 250 K for 2/3 Zn.

From our results we see that the formation of the intermediate MgB<sub>12</sub>H<sub>12</sub> is mainly responsible for the kinetic barrier, and methods to improve the kinetics of borohydrides should focus on reaction pathways avoiding the formation of this intermediate, as suggested by several other groups.<sup>17,18,47</sup> Because the kinetic barrier is roughly constant, at least for the full hydrogen release reaction, we do not expect alloying to have a direct impact on the height of the kinetic barrier. But, it is really the overall energy required to start the hydrogen desorption that is of interest—and that linearly decreases with Zn concentration. Note that the reaction kinetics can, at least in principle, be accelerated by using catalysts or by controlling the particle size of reactants.<sup>9</sup> Furthermore, it is also conceivable that the kinetics of the dehydrogenation reaction can be influenced by the inclusion of impurities, as studied by van de Walle’s group.<sup>13</sup>

## IV. CONCLUSIONS

In summary, *ab initio* calculations were performed to accurately determine formation enthalpies for many different materials suspected in the decomposition of Mg(BH<sub>4</sub>)<sub>2</sub>, to find reaction enthalpies for the most likely reaction pathways, and to study the effect of Zn concentration on the overall desorption reaction. We find that the overall thermodynamics of the desorption reaction can be optimized by alloying Mg(BH<sub>4</sub>)<sub>2</sub> with around 33% Zn. We estimate that in this case the temperature for the complete decomposition reaction is lowered by 123 K. Verifying the kinetics explicitly through *ab initio* calculations is difficult and is the subject of ongoing research. Supported by encouraging experimental results,<sup>20,29</sup> we conclude that alloying Mg(BH<sub>4</sub>)<sub>2</sub> with Zn is an ideal option for fine-tuning the desorption reaction without sacrificing too much gravimetric storage density.

## ACKNOWLEDGMENTS

This work was supported in full by NSF Grant No. DMR-1145968.

### Appendix A: Standard enthalpies of formation

We give here standard enthalpies of formations for all structures used throughout the main manuscript, calculated from DFT ground-state energies with temperature and zero-point contributions included through Eq. (3). Units of temperature  $T$  and enthalpy  $\Delta H$  are given in K and kJ/mol, respectively. We used experimental data for the temperature contributed enthalpy of H<sub>2</sub> gas.<sup>40</sup>

1. MgB<sub>2</sub>

$T$ [K]	$\Delta H$ [kJ/mol]	$T$ [K]	$\Delta H$ [kJ/mol]	$T$ [K]	$\Delta H$ [kJ/mol]	$T$ [K]	$\Delta H$ [kJ/mol]
25	-42.8478	225	-43.5773	425	-43.0847	625	-42.5631
50	-42.9136	250	-43.5474	450	-43.0123	650	-42.5079
75	-43.0676	275	-43.5007	475	-42.9416	675	-42.4547
100	-43.2423	300	-43.4422	500	-42.8729	700	-42.4035
125	-43.3909	325	-43.3760	525	-42.8063	725	-42.3542
150	-43.4969	350	-43.3053	550	-42.7421	750	-42.3067
175	-43.5594	375	-43.2321	575	-42.6802	775	-42.2608
200	-43.5837	400	-43.1582	600	-42.6205	800	-42.2166

$$\Delta H(T = 0) = -42.8445 \text{ kJ/mol}$$

$$\Delta H(E \text{ only}) = -41.3923 \text{ kJ/mol}$$

2. MgH<sub>2</sub>

$T$ [K]	$\Delta H$ [kJ/mol]	$T$ [K]	$\Delta H$ [kJ/mol]	$T$ [K]	$\Delta H$ [kJ/mol]	$T$ [K]	$\Delta H$ [kJ/mol]
25	-71.2620	225	-77.1642	425	-80.2792	625	-80.6338
50	-72.0536	250	-77.7319	450	-80.4525	650	-80.5411
75	-72.8916	275	-78.2442	475	-80.5836	675	-80.4248
100	-73.7396	300	-78.7003	500	-80.6754	700	-80.2867
125	-74.4942	325	-79.1201	525	-80.7307	725	-80.1277
150	-75.2186	350	-79.4855	550	-80.7519	750	-79.9499
175	-75.9036	375	-79.7983	575	-80.7413	775	-79.7546
200	-76.5428	400	-80.0609	600	-80.7012	800	-79.5430

$$\Delta H(T = 0) = -70.5096 \text{ kJ/mol}$$

$$\Delta H(E \text{ only}) = -80.7888 \text{ kJ/mol}$$

3. MgB<sub>12</sub>H<sub>12</sub>

$T$ [K]	$\Delta H$ [kJ/mol]	$T$ [K]	$\Delta H$ [kJ/mol]	$T$ [K]	$\Delta H$ [kJ/mol]	$T$ [K]	$\Delta H$ [kJ/mol]
25	-474.2918	225	-503.3760	425	-523.9349	625	-532.7084
50	-478.3169	250	-506.6553	450	-525.6071	650	-533.1555
75	-482.1853	275	-509.7199	475	-527.0971	675	-533.4792
100	-486.0506	300	-512.5552	500	-528.4145	700	-533.6845
125	-489.5086	325	-515.2722	525	-529.5698	725	-533.7732
150	-493.0109	350	-517.7585	550	-530.5696	750	-533.7528
175	-496.5009	375	-520.0212	575	-531.4215	775	-533.6277
200	-499.9106	400	-522.0699	600	-532.1323	800	-533.4021

$$\Delta H(T = 0) = -469.9027 \text{ kJ/mol}$$

$$\Delta H(E \text{ only}) = -612.5082 \text{ kJ/mol}$$

4. MgB<sub>4</sub>

$T$ [K]	$\Delta H$ [kJ/mol]	$T$ [K]	$\Delta H$ [kJ/mol]	$T$ [K]	$\Delta H$ [kJ/mol]	$T$ [K]	$\Delta H$ [kJ/mol]
25	-53.5246	225	-53.8921	425	-53.8095	625	-53.6442
50	-53.5565	250	-53.8964	450	-53.7899	650	-53.6232
75	-53.6239	275	-53.8942	475	-53.7698	675	-53.6023
100	-53.6993	300	-53.8869	500	-53.7492	700	-53.5815
125	-53.7661	325	-53.8758	525	-53.7284	725	-53.5607
150	-53.8183	350	-53.8619	550	-53.7074	750	-53.5401
175	-53.8554	375	-53.8458	575	-53.6864	775	-53.5196
200	-53.8792	400	-53.8282	600	-53.6653	800	-53.4992

$$\Delta H(T = 0) = -53.5227 \text{ kJ/mol}$$

$$\Delta H(E \text{ only}) = -53.8811 \text{ kJ/mol}$$

### 5. Zn-alloyed $\text{Mg}(\text{BH}_4)_2$

Values are given for all 10 alloying levels of  $\text{Mg}(\text{BH}_4)_2$  from 0/9 to 9/9. Units for temperature  $T$  and enthalpies  $\Delta H$  are K and kJ/mol, respectively.

$T$	$\Delta H(0/9)$	$\Delta H(1/9)$	$\Delta H(2/9)$	$\Delta H(3/9)$	$\Delta H(4/9)$	$\Delta H(5/9)$	$\Delta H(6/9)$	$\Delta H(7/9)$	$\Delta H(8/9)$	$\Delta H(9/9)$
$E_{\text{only}}$	-261.7976	-236.4970	-210.9513	-185.1490	-159.9197	-133.7350	-108.8261	-83.6754	-58.5632	-34.6722
0	-181.1409	-156.6974	-131.9971	-107.1175	-82.8319	-57.5765	-33.5969	-9.4840	14.9718	37.8973
25	-184.1121	-159.6661	-134.9744	-110.0966	-85.8174	-60.5598	-36.5847	-12.4716	11.9706	34.8856
50	-186.9262	-162.4711	-137.7886	-112.9080	-88.6331	-63.3640	-39.3886	-15.2746	9.1561	32.0606
75	-189.5518	-165.0799	-140.3934	-115.4973	-91.2175	-65.9289	-41.9403	-17.8210	6.6122	29.5198
100	-191.9842	-167.4923	-142.7930	-117.8747	-93.5821	-68.2694	-44.2600	-20.1315	4.3123	27.2310
125	-193.9260	-169.4133	-144.6961	-119.7533	-95.4431	-70.1046	-46.0719	-21.9319	2.5255	25.4591
150	-195.7116	-171.1788	-146.4412	-121.4734	-97.1444	-71.7801	-47.7249	-23.5728	0.8988	23.8480
175	-197.3677	-172.8158	-148.0571	-123.0648	-98.7177	-73.3288	-49.2532	-25.0893	-0.6041	22.3604
200	-198.9169	-174.3473	-149.5675	-124.5518	-100.1878	-74.7759	-50.6822	-26.5069	-2.0090	20.9701
225	-200.5059	-175.9197	-151.1194	-126.0814	-101.7016	-76.2683	-52.1583	-27.9718	-3.4620	19.5312
250	-202.0122	-177.4102	-152.5902	-127.5308	-103.1361	-77.6828	-53.5577	-29.3599	-4.8388	18.1682
275	-203.4391	-178.8220	-153.9828	-128.9030	-104.4940	-79.0218	-54.8824	-30.6729	-6.1412	16.8799
300	-204.7866	-180.1550	-155.2971	-130.1978	-105.7747	-80.2844	-56.1313	-31.9097	-7.3677	15.6677
325	-206.1304	-181.4847	-156.6087	-131.4905	-107.0534	-81.5459	-57.3793	-33.1450	-8.5931	14.4568
350	-207.3915	-182.7322	-157.8386	-132.7021	-108.2511	-82.7269	-58.5470	-34.2996	-9.7381	13.3268
375	-208.5682	-183.8955	-158.9848	-133.8306	-109.3658	-83.8256	-59.6324	-35.3715	-10.8005	12.2795
400	-209.6592	-184.9734	-160.0461	-134.8747	-110.3961	-84.8403	-60.6339	-36.3591	-11.7789	11.3164
425	-210.6765	-185.9779	-161.0344	-135.8465	-111.3540	-85.7832	-61.5637	-37.2747	-12.6855	10.4253
450	-211.6066	-186.8955	-161.9364	-136.7324	-112.2263	-86.6409	-62.4083	-38.1048	-13.5068	9.6196
475	-212.4497	-187.7263	-162.7521	-137.5326	-113.0128	-87.4133	-63.1678	-38.8497	-14.2430	8.8989
500	-213.2061	-188.4708	-163.4819	-138.2475	-113.7141	-88.1010	-63.8425	-39.5098	-14.8946	8.2629
525	-213.8777	-189.1306	-164.1276	-138.8788	-114.3320	-88.7056	-64.4344	-40.0870	-15.4635	7.7095
550	-214.4644	-189.7059	-164.6892	-139.4265	-114.8665	-89.2273	-64.9435	-40.5814	-15.9497	7.2385
575	-214.9676	-190.1980	-165.1681	-139.8920	-115.3189	-89.6673	-65.3711	-40.9945	-16.3547	6.8486
600	-215.3889	-190.6084	-165.5658	-140.2768	-115.6908	-90.0273	-65.7189	-41.3278	-16.6801	6.5381
625	-215.7300	-190.9390	-165.8841	-140.5827	-115.9840	-90.3089	-65.9885	-41.5831	-16.9276	6.3052
650	-215.9928	-191.1914	-166.1248	-140.8114	-116.2003	-90.5139	-66.1818	-41.7623	-17.0992	6.1480
675	-216.1793	-191.3679	-166.2899	-140.9650	-116.3418	-90.6445	-66.3009	-41.8675	-17.1969	6.0644
700	-216.2917	-191.4705	-166.3815	-141.0455	-116.4104	-90.7026	-66.3477	-41.9007	-17.2227	6.0522
725	-216.3300	-191.4993	-166.3998	-141.0531	-116.4063	-90.6884	-66.3225	-41.8621	-17.1769	6.1115
750	-216.2986	-191.4587	-166.3489	-140.9920	-116.3338	-90.6061	-66.2294	-41.7559	-17.0636	6.2378
775	-216.1996	-191.3507	-166.2312	-140.8643	-116.1951	-90.4578	-66.0707	-41.5843	-16.8850	6.4290
800	-216.0355	-191.1778	-166.0488	-140.6724	-115.9924	-90.2459	-65.8486	-41.3496	-16.6435	6.6828



**Appendix B: Absolute entropies**

Eq. (4). Units for temperature  $T$  and entropies  $S$  are K and J/K/mol, respectively.

We give here absolute entropies for all structures used throughout the main manuscript, calculated using

**1. MgB<sub>2</sub>**

$T$ [K]	$S$ [J/K/mol]	$T$ [K]	$S$ [J/K/mol]	$T$ [K]	$S$ [J/K/mol]	$T$ [K]	$S$ [J/K/mol]
25	0.0049	225	23.2048	425	55.1436	625	79.7405
50	0.2642	250	27.5212	450	58.6030	650	82.3799
75	1.4697	275	31.7893	475	61.9427	675	84.9384
100	3.7830	300	35.9743	500	65.1672	700	87.4202
125	6.9282	325	40.0539	525	68.2817	725	89.8290
150	10.6248	350	44.0151	550	71.2912	750	92.1687
175	14.6636	375	47.8514	575	74.2008	775	94.4427
200	18.8933	400	51.5607	600	77.0157	800	96.6542

**2. MgH<sub>2</sub>**

$T$ [K]	$S$ [J/K/mol]	$T$ [K]	$S$ [J/K/mol]	$T$ [K]	$S$ [J/K/mol]	$T$ [K]	$S$ [J/K/mol]
25	0.0301	225	21.1051	425	43.7259	625	63.4665
50	0.8668	250	24.0625	450	46.3667	650	65.7097
75	2.9991	275	26.9837	475	48.9595	675	67.9047
100	5.8224	300	29.8698	500	51.5030	700	70.0524
125	8.8840	325	32.7202	525	53.9965	725	72.1538
150	11.9888	350	35.5334	550	56.4395	750	74.2101
175	15.0695	375	38.3071	575	58.8319	775	76.2224
200	18.1085	400	41.0387	600	61.1741	800	78.1921

**3. MgB<sub>12</sub>H<sub>12</sub>**

$T$ [K]	$S$ [J/K/mol]	$T$ [K]	$S$ [J/K/mol]	$T$ [K]	$S$ [J/K/mol]	$T$ [K]	$S$ [J/K/mol]
25	6.3137	225	120.6799	425	270.7316	625	415.3139
50	20.9873	250	137.9110	450	289.7719	650	431.9936
75	35.4722	275	155.9381	475	308.5848	675	448.3569
100	48.9467	300	174.5592	500	327.1345	700	464.4084
125	61.9336	325	193.5822	525	345.3956	725	480.1542
150	75.1936	350	212.8384	550	363.3518	750	495.6008
175	89.2742	375	232.1869	575	380.9930	775	510.7553
200	104.4286	400	251.5141	600	398.3141	800	525.6249

**4. MgB<sub>4</sub>**

$T$ [K]	$S$ [J/K/mol]	$T$ [K]	$S$ [J/K/mol]	$T$ [K]	$S$ [J/K/mol]	$T$ [K]	$S$ [J/K/mol]
25	0.0637	225	34.4447	425	80.6957	625	118.8385
50	1.1818	250	40.4270	450	85.9533	650	123.0205
75	3.8995	275	46.4271	475	91.0663	675	127.0873
100	7.7271	300	52.3932	500	96.0356	700	131.0436
125	12.2816	325	58.2867	525	100.8636	725	134.8940
150	17.3581	350	64.0798	550	105.5537	750	138.6430
175	22.8185	375	69.7532	575	110.1098	775	142.2949
200	28.5473	400	75.2944	600	114.5366	800	145.8538

### 5. Zn-alloyed $\text{Mg}(\text{BH}_4)_2$

Values are given for all 10 alloying levels of  $\text{Mg}(\text{BH}_4)_2$  from 0/9 to 9/9. Units for temperature  $T$  and entropy  $S$  are K and J/K/mol, respectively.

$T$	$S(0/9)$	$S(1/9)$	$S(2/9)$	$S(3/9)$	$S(4/9)$	$S(5/9)$	$S(6/9)$	$S(7/9)$	$S(8/9)$	$S(9/9)$
25	1.6220	2.2841	2.2170	2.6043	2.7088	3.3761	3.5663	4.1165	3.6454	3.4832
50	8.3785	9.8673	10.1158	11.1473	11.7055	13.2631	14.0306	15.1895	14.9646	15.0737
75	18.0017	20.0819	20.7124	22.3144	23.2698	25.4639	26.7622	28.3285	28.4614	28.9387
100	28.7955	31.2783	32.2271	34.2544	35.5285	38.1711	39.8800	41.7232	42.1489	42.9248
125	39.9059	42.6715	43.8770	46.2207	47.7481	50.7195	52.7340	54.7764	55.4214	56.4269
150	50.9458	53.9177	55.3307	57.9162	59.6395	62.8582	65.0962	67.2857	68.0931	69.2724
175	61.7268	64.8542	66.4356	69.2103	71.0836	74.4918	76.8938	79.1943	80.1235	81.4350
200	72.1649	75.4130	77.1325	80.0582	82.0477	85.6044	88.1291	90.5164	91.5394	92.9545
225	82.2382	85.5830	87.4171	90.4661	92.5482	96.2238	98.8438	101.3023	102.3994	103.8990
250	91.9590	95.3833	97.3144	100.4663	102.6246	106.3980	109.0946	111.6142	112.7719	114.3435
275	101.3544	104.8461	106.8603	110.0999	112.3230	116.1785	118.9395	121.5135	122.7219	124.3569
300	110.4554	114.0053	116.0920	119.4075	121.6873	125.6133	128.4297	131.0536	132.3055	133.9978
325	119.2913	122.8923	125.0430	128.4251	130.7555	134.7429	137.6085	140.2788	141.5685	143.3135
350	127.8875	131.5339	133.7417	137.1828	139.5591	143.6006	146.5106	149.2246	150.5477	152.3417
375	136.2653	139.9525	142.2114	145.7053	148.1238	152.2135	155.1640	157.9193	159.2723	161.1119
400	144.4423	148.1666	150.4716	154.0130	156.4703	160.6034	163.5911	166.3856	167.7655	169.6480
425	152.4333	156.1913	158.5381	162.1224	164.6158	168.7881	171.8103	174.6419	176.0464	177.9691
450	160.2505	164.0394	166.4242	170.0474	172.5745	176.7823	179.8367	182.7035	184.1304	186.0909
475	167.9043	171.7216	174.1411	177.7996	180.3582	184.5984	187.6828	190.5831	192.0306	194.0267
500	175.4037	179.2471	181.6983	185.3892	187.9771	192.2471	195.3595	198.2915	199.7581	201.7877
525	182.7562	186.6239	189.1041	192.8245	195.4401	199.7373	202.8760	205.8380	207.3223	209.3835
550	189.9688	193.8589	196.3658	200.1133	202.7547	207.0769	210.2403	213.2308	214.7316	216.8225
575	197.0471	200.9582	203.4895	207.2619	209.9277	214.2730	217.4595	220.4770	221.9932	224.1120
600	203.9967	207.9271	210.4811	214.2763	216.9650	221.3316	224.5399	227.5829	229.1135	231.2586
625	210.8220	214.7706	217.3453	221.1617	223.8719	228.2583	231.4870	234.5542	236.0983	238.2681
650	217.5274	221.4929	224.0869	227.9228	230.6532	235.0579	238.3058	241.3958	242.9527	245.1457
675	224.1166	228.0979	230.7098	234.5638	237.3132	241.7350	245.0009	248.1126	249.6814	251.8963
700	230.5933	234.5894	237.2179	241.0885	243.8558	248.2935	251.5764	254.7085	256.2887	258.5241
725	236.9606	240.9707	243.6144	247.5006	250.2848	254.7373	258.0361	261.1876	262.7785	265.0332
750	243.2216	247.2447	249.9027	253.8033	256.6034	261.0697	264.3836	267.5534	269.1543	271.4272
775	249.3791	253.4144	256.0858	259.9998	262.8148	267.2940	270.6221	273.8092	275.4197	277.7096
800	255.4358	259.4825	262.1663	266.0928	268.9220	273.4133	276.7547	279.9581	281.5777	283.8837

### 6. Mg

$T$ [K]	$S$ [J/K/mol]	$T$ [K]	$S$ [J/K/mol]	$T$ [K]	$S$ [J/K/mol]	$T$ [K]	$S$ [J/K/mol]
25	0.1591	225	25.4974	425	40.3539	625	49.6940
50	2.0640	250	27.8794	450	41.7287	650	50.6506
75	5.6107	275	30.0685	475	43.0327	675	51.5719
100	9.5667	300	32.0909	500	44.2727	700	52.4604
125	13.3697	325	33.9685	525	45.4546	725	53.3183
150	16.8606	350	35.7196	550	46.5835	750	54.1477
175	20.0248	375	37.3593	575	47.6638	775	54.9504
200	22.8912	400	38.9005	600	48.6995	800	55.7281

## 7. B

$T$ [K]	$S$ [J/K/mol]	$T$ [K]	$S$ [J/K/mol]	$T$ [K]	$S$ [J/K/mol]	$T$ [K]	$S$ [J/K/mol]
25	0.0000	225	3.3007	425	11.0926	625	18.2138
50	0.0061	250	4.2054	450	12.0522	650	19.0120
75	0.0690	275	5.1561	475	12.9935	675	19.7904
100	0.2541	300	6.1357	500	13.9153	700	20.5498
125	0.5915	325	7.1308	525	14.8167	725	21.2906
150	1.0835	350	8.1310	550	15.6972	750	22.0135
175	1.7150	375	9.1284	575	16.5568	775	22.7191
200	2.4626	400	10.117	600	17.3956	800	23.4080

## 8. Zn

$T$ [K]	$S$ [J/K/mol]	$T$ [K]	$S$ [J/K/mol]	$T$ [K]	$S$ [J/K/mol]	$T$ [K]	$S$ [J/K/mol]
25	4.7968	225	42.0395	425	57.3580	625	66.7984
50	12.0016	250	44.5407	450	58.7529	650	67.7615
75	18.4567	275	46.8192	475	60.0739	675	68.6886
100	23.9634	300	48.9104	500	61.3285	700	69.5823
125	28.6435	325	50.8420	525	62.5229	725	70.4450
150	32.6659	350	52.6362	550	63.6627	750	71.2786
175	36.1722	375	54.3109	575	64.7525	775	72.0851
200	39.2701	400	55.8807	600	65.7965	800	72.8662

\* thonhauser@wfu.edu

- <sup>1</sup> J. Graetz, Chem. Soc. Rev. **38**, 73 (2009).
- <sup>2</sup> E. Rönnebro, Curr. Opin. Solid State Mater. Sci. **15**, 44 (2011).
- <sup>3</sup> H.-W. Li, Y. Yan, S.-i. Orimo, A. Züttel, and C. M. Jensen, Energies **4**, 185 (2011).
- <sup>4</sup> L. H. Rude, T. K. Nielsen, D. B. Ravensbaek, U. Bösenberg, M. B. Ley, B. Richter, L. M. Arnbjerg, M. Dornheim, Y. Filinchuk, F. Besenbacher, and T. R. Jensen, Phys. Status Solidi A **208**, 1754 (2011).
- <sup>5</sup> I. P. Jain, P. Jain, and A. Jain, J. Alloys Compd. **503**, 303 (2010).
- <sup>6</sup> DOE Targets for Onboard Hydrogen Storage Systems for Light-Duty Vehicles, retrieved from [http://energy.gov/sites/prod/files/2014/03/f12/targets\\_onboard\\_hydro\\_storage.pdf](http://energy.gov/sites/prod/files/2014/03/f12/targets_onboard_hydro_storage.pdf) (US Department of Energy, 2009) – for a good side-by-side comparison between the old and new DOE targets see Ref. [7].
- <sup>7</sup> J. Yang, A. Sudik, C. Wolverton, and D. J. Siegel, Chem. Soc. Rev. **39**, 656 (2010).
- <sup>8</sup> J. J. Vajo, S. L. Skeith, and F. Mertens, J. Phys. Chem. B **109**, 3719 (2005).
- <sup>9</sup> S. V. Alapati, K. J. Johnson, and D. S. Sholl, Phys. Chem. Chem. Phys. **9**, 1438 (2007).
- <sup>10</sup> S. V. Alapati, J. K. Johnson, and D. S. Sholl, J. Phys. Chem. C **112**, 5258 (2008).
- <sup>11</sup> H.-W. Li, K. Kikuchi, Y. Nakamori, N. Ohba, K. Miwa, S. Towata, and S. Orimo, Acta Mater. **56**, 1342 (2008).
- <sup>12</sup> E. A. Nickels, M. O. Jones, W. I. F. David, S. R. Johnson, R. L. Lowton, M. Sommariva, and P. P. Edwards, Angew. Chemie Int. Ed. **47**, 2817 (2008).
- <sup>13</sup> K. Hoang and C. G. Van de Walle, Phys. Rev. B **80**, 214109 (2009).
- <sup>14</sup> M. J. van Setten, G. A. de Wijs, and G. Brocks, Phys. Rev. B **76**, 075125 (2007).
- <sup>15</sup> H. W. Brinks, A. Fossdal, and B. C. Hauback, J. Phys. Chem. C **112**, 5658 (2008).
- <sup>16</sup> H.-W. Li, K. Kikuchi, Y. Nakamori, K. Miwa, S. Towata, and S. Orimo, Scr. Mater. **57**, 679 (2007).
- <sup>17</sup> G. Severa, E. Rönnebro, and C. M. Jensen, Chem. Commun. **46**, 421 (2010).
- <sup>18</sup> G. L. Soloveichik, Y. Gao, J. Rijssenbeek, M. Andrus, S. Kniajanski, R. C. Bowman, Jr., S.-J. Hwang, and J.-C. Zhao, Int. J. Hydrogen Energy **34**, 916 (2009).
- <sup>19</sup> V. Ozoliņš, E. H. Majzoub, and C. Wolverton, Phys. Rev. Lett. **100**, 135501 (2008).
- <sup>20</sup> E. Albanese, G. N. Kalantzopoulos, J. G. Vitillo, E. Pina-tel, B. Civalleri, S. Deledda, S. Bordiga, B. C. Hauback, and M. Baricco, J. Alloys Compd. **580**, S282 (2013).
- <sup>21</sup> Y. Zhang, E. Majzoub, V. Ozoliņš, and C. Wolverton, J. Phys. Chem. C **116**, 10522 (2012).
- <sup>22</sup> M. J. van Setten, G. A. de Wijs, M. Fichtner, and G. Brocks, Chem. Mater. **20**, 4952 (2008).
- <sup>23</sup> T. D. Huan, M. Amsler, R. Sabatini, V. N. Tuoc, N. B. Le, L. M. Woods, N. Marzari, and S. Goedecker, Phys. Rev. B **88**, 024108 (2013).
- <sup>24</sup> A. Bil, B. Kolb, R. Atkinson, D. G. Pettifor, T. Thonhauser, and A. N. Kolmogorov, Phys. Rev. B **83**, 224103 (2011).
- <sup>25</sup> Y. Nakamori, K. Miwa, A. Ninomiya, H. Li, N. Ohba, S. I. Towata, A. Züttel, and S. I. Orimo, Phys. Rev. B **74**, 045126 (2006).

- <sup>26</sup> Using the entire experimental data from Ref. 27 on all borohydrides yields a fit of  $T_d = 1435 - 675.0\chi_P$  and  $T_d = 439.4 + 6.71\Delta H_f$ . The fits here were obtained by limiting the experimental data to all borohydrides with double-valence metals.
- <sup>27</sup> Y. Nakamori, H.-W. Li, K. Kikuchi, M. Aoki, K. Miwa, S. Towata, and S. Orimo, *J. Alloys Compd.* **446-447**, 296 (2007).
- <sup>28</sup> E. Jeon and Y. Cho, *J. Alloys Compd.* **422**, 273 (2006).
- <sup>29</sup> G. N. Kalantzopoulos, J. G. Vitillo, E. Albanese, E. Pinatell, B. Civalieri, S. Deledda, S. Bordiga, M. Baricco, and B. C. Hauback, *J. Alloys Compd.* , 10 (2014), in press.
- <sup>30</sup> D. Ravnsbaek, Y. Filinchuk, Y. Cerenius, H. J. Jakobsen, F. Besenbacher, J. Skibsted, and T. R. Jensen, *Angew. Chemie Int. Ed.* **48**, 6659 (2009).
- <sup>31</sup> K. Miwa, N. Ohba, S. Towata, Y. Nakamori, and S. Orimo, *J. Alloys Compd.* **404-406**, 140 (2005).
- <sup>32</sup> G. Kresse and J. Furthmüller, *Phys. Rev. B* **54**, 11169 (1996).
- <sup>33</sup> G. Kresse and D. Joubert, *Phys. Rev. B* **59**, 1758 (1999).
- <sup>34</sup> M. J. van Setten, M. A. Uijttewaai, G. A. de Wijs, and R. A. de Groot, *J. Am. Chem. Soc.* **129**, 2458 (2007).
- <sup>35</sup> Z. Lodziana, *Phys. Rev. B* **81**, 144108 (2010).
- <sup>36</sup> T. Thonhauser, V. R. Cooper, S. Li, A. Puzder, P. Hyldgaard, and D. C. Langreth, *Phys. Rev. B* **76**, 125112 (2007).
- <sup>37</sup> D. C. Langreth, B. I. Lundqvist, S. D. Chakarova-Käck, V. R. Cooper, M. Dion, P. Hyldgaard, A. Kelkkanen, J. Kleis, L. Kong, S. Li, P. G. Moses, E. D. Murray, A. Puzder, H. Rydberg, E. Schröder, and T. Thonhauser, *J. Phys. Condens. Matter* **21**, 084203 (2009).
- <sup>38</sup> M. Dion, H. Rydberg, E. Schröder, D. C. Langreth, and B. I. Lundqvist, *Phys. Rev. Lett.* **92**, 246401 (2004).
- <sup>39</sup> G. Henkelman, A. Arnaldsson, and H. Jónsson, *Comput. Mat. Sci.* **36**, 254 (2006).
- <sup>40</sup> H. Hemmes, A. Driessen, and R. Griessen, *J. Phys. C* **19**, 3571 (1986).
- <sup>41</sup> Y. Yan, H.-W. Li, Y. Nakamori, N. Ohba, K. Miwa, S.-i. Towata, and S.-i. Orimo, *Mater. Trans.* **49**, 2751 (2008).
- <sup>42</sup> J. J. Vajo, F. Mertens, C. C. Ahn, R. C. Bowman, and B. Fultz, *J. Phys. Chem. B* **108**, 13977 (2004).
- <sup>43</sup> G. Balducci, S. Brutti, A. Ciccioli, G. Gigli, P. Manfrinetti, A. Palenzona, M. F. Butman, and L. Kudin, *J. Phys. Chem. Solids* **66**, 292 (2005).
- <sup>44</sup> The authors of Ref. [41] propose here the decomposition of  $\text{MgB}_{12}\text{H}_{12}$  before  $\text{MgH}_2$ , which we find to be unlikely as it has a critical temperature of 716 K. We suspect the actual reaction studied was the one we proposed.
- <sup>45</sup> V. Ozoliņš, E. H. Majzoub, and C. Wolverton, *J. Am. Chem. Soc.* **131**, 230 (2009).
- <sup>46</sup> R. J. Newhouse, V. Stavila, S.-J. Hwang, L. E. Klebanoff, and J. Z. Zhang, *J. Phys. Chem. C* **114**, 5224 (2010).
- <sup>47</sup> Y. Yan, H.-W. Li, H. Maekawa, M. Aoki, T. Noritake, M. Matsumoto, K. Miwa, S.-i. Towata, and S.-i. Orimo, *Mater. Trans.* **52**, 1443 (2011).
- <sup>48</sup> J. Yang, X. Zhang, J. Zheng, P. Song, and X. Li, *Scripta Mater.* **64**, 225 (2011).
- <sup>49</sup> Y. Zhang, E. Majzoub, V. Ozoliņš, and C. Wolverton, *Phys. Rev. B* **82**, 174107 (2010).
- <sup>50</sup> T. Matsunaga, F. Buchter, P. Mauron, M. Bielman, Y. Nakamori, S. Orimo, N. Ohba, K. Miwa, S. Towata, and A. Züttel, *J. Alloys Compd.* **459**, 583 (2008).
- <sup>51</sup> A. Züttel, P. Wenger, S. Rentsch, P. Sudan, P. Mauron, and C. Emmenegger, *J. Power Sources* **118**, 1 (2003).